Energy Dependence of Proton Damage in AlGaAs Light-Emitting Diodes

Robert A. Reed, *Member, IEEE*, Paul W. Marshall, *Member, IEEE*, Cheryl J. Marshall, *Member, IEEE*, Ray L. Ladbury, Hak S. Kim, *Member, IEEE*, Loc Xuan Nguyen, Janet L. Barth, *Senior Member, IEEE*, and Kenneth A. LaBel, *Member, IEEE*

***Abstract*—We measure the energy dependence of proton-induced LED degradation using large numbers of devices and incremental exposures to gain high confidence in the proton energy dependence and device-to-device variability of damage. We compare single versus double heterojunction AlGaAs technologies (emitting at 880 nm and 830 nm, respectively) to previous experimental and theoretical results. We also present a critical review of the use of nonionizing energy loss in AlGaAs for predictions of on-orbit degradation and assess the uncertainties inherent in this approach.**

I. Introduction

A DETAILED understanding of proton-induced degradation in modern light-emitting diode (LED) technologies is paramount to assessing their reliability in optocoupler structures and in other applications common to many satellite designs. Our study addresses the need to develop an understanding of the types of structures and material systems that exhibit tolerance to proton degradation, and the need to gain confidence in our test methods and models for applying laboratory studies to calculate the anticipated device response in a given proton environment. We focus on LED technologies that are commonly found in commercially available devices since they are the most practical option for satellite designers.

Barnes and coworkers were among the first to recognize the degradation mechanisms and relative sensitivities of GaAs based LED structures. They reported their findings in [1]–[3] where they described the role of displacement damage in degrading the carrier lifetime and introducing defects that allow nonradiative recombination that competes with the desired radiative recombination process. In particular, they identify amphoterically doped LED structures as being especially sensitive to these effects. More recently, several groups [4]–[7] have extended these studies to current LED technologies (some used in optocouplers) and confirmed that amphoterically doped devices appear to be much more sensitive to proton displacement effects than heterostructure based approaches. In [4] it was noted that longer wavelength (890 nm) AlGaAs amphoteric LEDs were particularly sensitive and resulted in optocoupler failure on the TOPEX satellite. Our study extends these investigations by comparing single versus double heterostructure AlGaAs LED devices (emitting at 880 nm and 830 nm, respectively) to assess their tolerance to protons.

The extension of accelerator-based proton degradation test data to predict on-orbit performance of a given optocoupler or LED technology requires good knowledge of the energy dependence of proton damage and careful selection of the proton test energy or energies. As we discuss in Section II, studies of the utility of the energy dependence of the NonIonizing Energy Loss (NIEL) for protons in GaAs-based devices have not all supported the use of the NIEL as an appropriate metric for describing the energy dependence of damage in III–V devices. Therefore, a second major objective of our study addresses this as yet unresolved issue by conducting an extensive investigation of the proton energy dependence of AlGaAs LEDs over the proton energy range from 10 MeV to 500 MeV. By relying on large numbers of devices and 5 or greater exposure increments at a given energy, we assure that the trends noted are statistically significant and also arrive at a measure of the device-to-device dependence of the measured damage factors.

II. NIEL and GaAs Structures

In order to calculate the expected radiation response of a device in a proton environment, it is necessary to measure or make assumptions on the energy dependence for the performance parameter of interest. This is important because flight programs typically expect on-orbit performance predictions based on measurements made at a single or a few energies. For device properties that degrade primarily as a result of displacement damage, one typically uses the calculated NIEL as a function of incident proton energy for the relevant material. In the case of GaAs (and related compounds) this approach entails significant uncertainty because of observed deviations between the NIEL energy dependence and those observed experimentally [8].

Deviations at very low proton energies (approaching the displacement energy thresholds) are expected [9], [10], but they are not generally of concern for proton applications in shielded spacecraft components because they contribute little to the total displacement damage behind typical shielding. However, deviations from the energy dependence of the calculated NIEL have been observed GaAs (as well as Si) device measurements as discussed further in [11]. Depending on how the damage factor measurements were normalized to NIEL, the deviations have

Manuscript received September 29, 2000. This work was supported by NASA/Electronics Radiation Characterization Project and Defense Threat Reduction Agency Contract 00-3001.

R. A. Reed, P. W. Marshall, C. J. Marshall, J. L. Barth, and K. A. LaBel, are with NASA/Goddard Space Flight Center (GSFC), Code 562, Greenbelt, MD USA (e-mail: robert.reed@gsfc.nasa.gov).

R. L. Ladbury is with Orbital Sciences Corporation, McLean, VA USA.

H. S. Kim is with Jackson and Tull Chartered Engineers, Washington, DC USA.

L. X. Nguyen is with Raytheon Information Technology and Sciences Services, Lanham, MD USA.

Publisher Item Identifier S 0018-9499(00)11177-3.

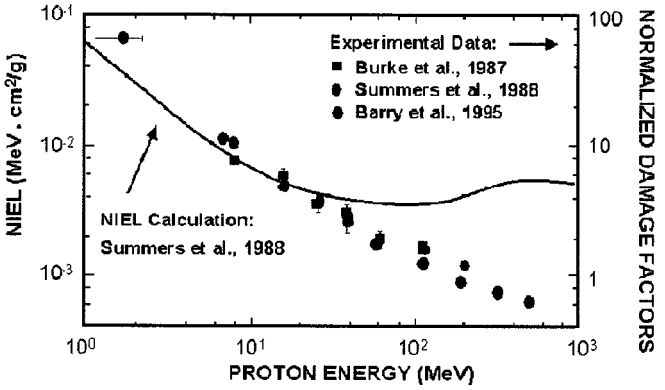

Fig. 1. Comparison of NIEL in GaAs (scaled to the left abscissa) to experimentally measured damage factors for GaAs related devices (scaled to the right abscissa and normalized to agree with the NIEL calculated value for 10 MeV protons). Divergence between the calculated and measured values is evident for proton energies over 50 MeV.

been reported either as over estimate of damage factors by the NIEL energy dependence at higher energies, or when the normalization is made at higher energies, being underestimated at the lower energies. The earliest energy dependent GaAs displacement damage factors were measured using J-FETs and resistors [12]–[14]. The damage factors deviated from NIEL at higher proton energies by falling below the calculated NIEL. However, the authors in [12] and [13] suggest the discrepancy as due to a lack of displacement damage equilibrium in the thin active regions near the surface of the devices (which were irradiated from the front), and conclude that the data should follow the NIEL energy dependence even at higher proton energies. Carlone *et al.* [14] conclude that the agreement between the calculated NIEL and experimental damage factors would improve at higher energies if the treatment of the inelastic scattering parameter is improved.

In contrast with these results, later experimental work by Luera *et al.* [15], Griffin *et al.* [16], Barry *et al.* [8], and the present paper, all indicate that lower energy protons are more effective at producing displacement damage in GaAs as compared to higher energy protons (in relation to predictions assuming damage correlates with NIEL). Luera *et al.* and Griffin *et al.*measured carrier removal damage factors in Van der Pauw samples and minority carrier lifetime degradation in LEDs resulting from neutron irradiation. Detailed calculations of the displacement kerma function were performed and the 14 MeV-to-reactor experimental damage ratios were smaller than predicted. The results were explained by variations in the recombination efficiency of the Frenkel pairs in the initial collision cascade as a function of Primary Knock-on Atom (PKA) energy [15]. Further discussion of Frenkel pair recombination may be found in ([9], [11], [8] and references therein).

To date, the most extensive set of GaAs damage constants is described in a 1995 paper by Barry *et al.*in which minority carrier lifetime damage factors in amphoterically doped GaAs LEDs were measured for proton energies as high as ~500 MeV [8]. In Fig. 1, the experimental results are compared with the NIEL calculation by Summers [13] by normalizing them at 10 MeV, and a clear discrepancy is observed in the 150–500 MeV range. (Note that Summers *et al.* [10] revised the NIEL calculation in 1993, there was very little difference between in the values computed for NIEL in the 1993 and that in the 1988 paper [13].) It is worthwhile noting that there are two photoluminescence studies performed on GaAs irradiated with protons in the same energy range [14], [15] that are also consistent with the results of Barry *et al.* [8]. In contrast, Lee *et al.* [17] present lifetime degradation measurements for various proton energies on a AlGaAs multiquantum-well laser diodes and show an apparent trend that somewhat consistent with NIEL. However, the authors conclude that the energy dependence is inconclusive due to the lack of statistics.

Finally, we note that the 1993 paper by Summers *et al.* [10] claims to have demonstrated a general linear correlation between device "proton damage coefficients" and NIEL for Si, GaAs and InP, using "solar cells as examples." Nevertheless, the data presented in that work do not cover the relevant range of proton energies for most satellite applications which are more heavily shielded. For example, both the GaAs data (from [18]) and the InP data (from [19]) are for protons below 20 MeV, and are indeed most relevant to lightly shielded solar cell applications. It is interesting to note that a recent paper based on the same solar cell data set [18], shows damage coefficients falling below the calculated GaAs NIEL at higher proton energies [20], consistent with Fig. 1.

In summary, there is a lack of consensus in the literature concerning the applicability of present NIEL calculations to describe the energy dependence of displacement damage factors in GaAs devices.

The remainder of this paper will present results of extensive energy-dependent damage-factor studies for both single and double heterojunction GaAs-based LEDs. We have undertaken a careful set of measurements on currently relevant commercial LEDs in an attempt to reduce the uncertainty in the use of NIEL to make space predictions for optocouplers and LEDs. Note that the total NIEL for a compound material such as AlGaAs is calculated by summing the contributions of each element weighted by its atomic fraction [21]. The results for $Al_{0.06}Ga_{0.94}As$ (estimated values for the double heterojunction LEDs used in this paper) are virtually identical to the GaAs NIEL.

III. Devices and Experimental Methods

In this study we evaluate a set of Single Heterojunction (SH) LEDs and a set of Double Heterojunction (DH) LEDs for proton sensitivity. The LEDs were provided by Isolink, Inc which manufactures optocouplers (the LED manufacture is proprietary). The double heterojunction LED is used in the OLH249 optocoupler and the single heterojunction LED is used in the 4N49 optocoupler. Fig. 2 gives a illustration of the different layers that form each type of LED. The two device types are described in Tables I and II. The die were mounted on a substrate that allowed for biasing of the LEDs. Seven LEDs were packaged on each substrate. Results for one vender lot of the single heterojunction LEDs and two vendor lots of the double heterojunction LEDs will be presented.

A step-irradiation approach was used to determine the proton-induced degradation of the LED output power. We

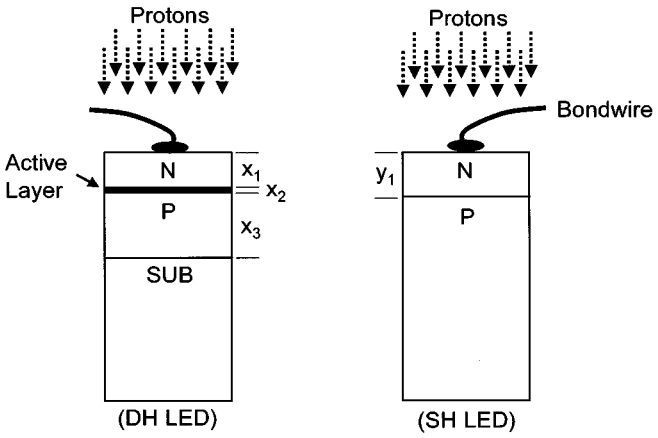

Fig. 2. Schematic illustration of the irradiation of a double-heterojunction LED (left) and a single-heterojunction LED (right).

TABLE I
DOUBLE HETEROJUNCTION LEDS

Wavelength	815 – 845 nm
Semiconductor	AlGaAs
N Region Dopant	Te
N Region Thickness (x_1)	40 – 80 μm
Active Layer Dopant	Zn
Active Layer Thickness (x_2)	0.5 – 2.0 μm
P Dopant	Zn
P Region Thickness (x_3)	10 – 40 μm
Overall LED Thickness	300 – 450 μm
Device obtained	LOT #3 – 18 LEDs LOT #4 – 191 LEDs

TABLE II
SINGLE HETEROJUNCTION LEDS

Wavelength	860 – 900 nm
Semiconductor	AlGaAs
N Region Dopant	Si
N Region Thickness (y_1)	50 – 110 μm
P Dopant	Zn
P Region Thickness (y_2)	130 – 250 μm
Device obtained	LOT #1 – 191 LEDs

simultaneously exposed a group of unbiased LEDs at each proton energy to specified fluence levels, and measured the LED output power after each exposure. Simultaneously exposing all LEDs at each energy resulted in minimizing uncertainty in the exposure levels. The largest uncertainty is the beam uniformity which is measured when necessary. A new group of LEDs was used for each proton energy.

The test setup allows for monitoring the output power of up to 21 LEDs independently. The output power was measured at various locations around each LED relative to the emitting surface of the LED. Fig. 3 shows a diagram of the test setup. An Externally Calibrated Photodetector (EPD) collected a portion of

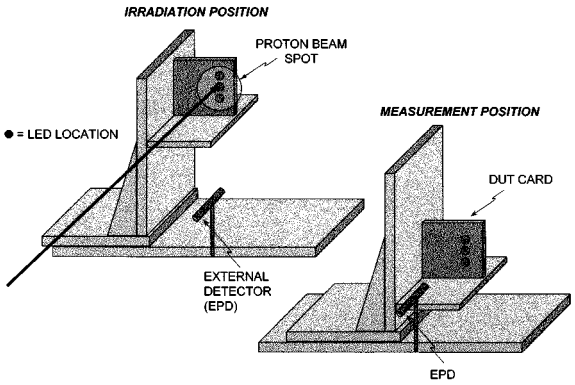

Fig. 3. Cartoon of stage movement between irradiation position and measurement position.

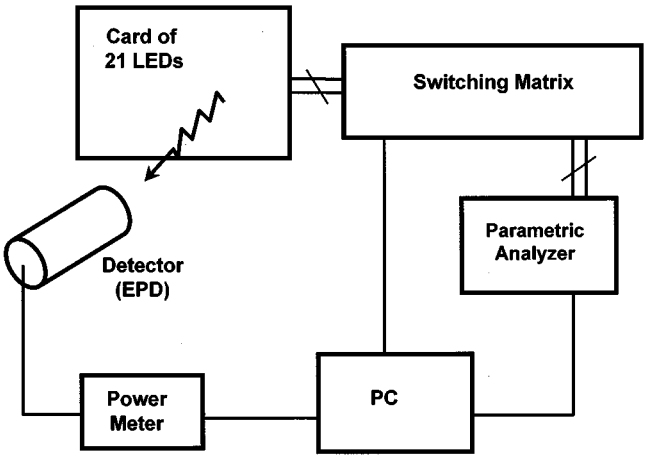

Fig. 4. Block diagram of experimental setup.

the LED output power. An x, y, z, θ (or 4D) stage was used to move the device between the detector and the proton beam and also to systematically map out the LED radiance field around the peak emission direction (x and θ are not shown in Fig. 3).

Fig. 4 shows a block diagram of the test setup. The 4D stage was used to map the output of the LED by moving the position of the LED relative to the EPD in small discrete steps. The EPD output is recorded as a function of relative position, giving a full mapping of the LED output power over position, see Fig. 5. The variation of the EPD output from maximum value (or peak position) to the minimum value position is less than a 50%, defining an "area" over which the LED output will be measured. For this study, the location that gives the peak value of the output power was used to compare the post-irradiation and pre-irradiation measurements. To ensure that the peak value was measured, a complete scan over each exposed LED was completed after each exposure.

Customized LAB VIEW® software provided a user interface to control signals to the LED and EPD. The software automatically monitors the EPD output and records each output power at each location to a file. In all cases LED forward current was held constant at 4 mA. The selection of this test condition was carefully chosen to represent a typical application current while minimizing device annealing as discussed below.

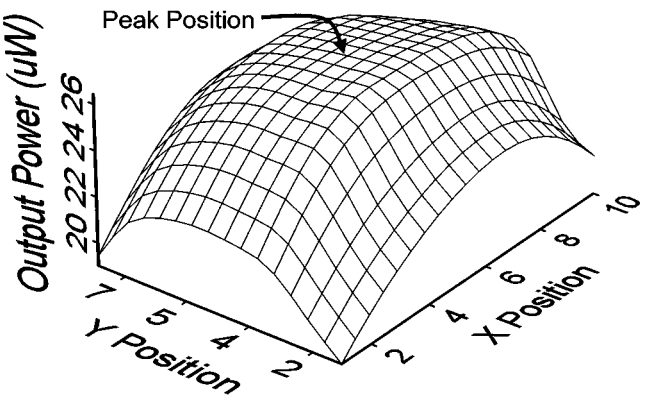

Fig. 5. Relative LED-EDP scan of measured LED output power. The output power value at the peak position was used in this study to determine the LED degradation.

There are several experimental issues that need careful attention when making LED measurements. We detail some of those below.

We ensured the repeatability of the LED output values after moving between the irradiation and the measurement positions by reproducing pre-irradiation measurements several times. The measurements were reproducible to better than 2%.

Injection current annealing can occur in LEDs [1], [7]. A study was completed to demonstrate that injection current annealing did not impact the LED output power measured during this study. These results showed that when the forward current is held at 4 mA and the total time the LED was biased was less than 10 minutes the injection current annealing was held to $<$12%. These results also showed that if the total on time was less than 1 min the injection current annealing was held to less than 3%. Typical measurement times were approximately 70 seconds, and therefore injection annealing had little effect on the determination of output degradation which was typically greater than 25% for a given exposure.

Stability of the LED output was verified prior to data collection. A study that measured the changes in output power just after an irradiation was conducted. We found that the LEDs stabilized in a few seconds. We also found that after irradiation the output power at 5 seconds and 30 seconds after applying bias were within 1.2%.

Beam dosimetry issues like flux uniformity, energy spreading at low energies, and accuracy across facilities were quantified. The latter two will be addressed later. The proton beam profiles were measured using radiation sensitive film for each proton energy. The film was used to determine the beam profile and the fluence was corrected all variations in beam uniformity across the exposure area. For all tests the cyclotron was tuned to the test energy, this reduced the uncertainty in beam energy.

The test facilities used were University of California at Davis Crocker Nuclear Laboratory (CNL) and Tri-University Meson Facility's (TRIUMF's) Proton Irradiation Facility (PIF). CNL proton energies were 63, 20 and 9.5 MeV. TRIUMF energies were 62, 225, 200, and 500 MeV. All energies at both facilities were achieved by tuning the cyclotron so that energy straggling of a degraded beam was not a concern.

A. Experimental Details for Single Heterojunction LEDs

The single heterojunction LEDs were exposed to 9.5, 20, 62, 63, 103, 200 and 500 MeV protons. For all energies all LEDs were exposed to between 8.5×10^{10} to 1×10^{11} p/cm^2. All beams were monitored for uniformity across the exposure area. This uniformity was within 10% for the 62, 63, 103, 200, and 500 MeV beams. The 9.5 and 20 MeV fluence data was corrected for the nonuniformity.

Using TRIM we estimate the spread in the proton energy due to shadowing from 1.3 mil gold bond wires, gold bonds, and the AlGaAs 50–110 μm N region epi-layer. For the 9.5 MeV proton beam, approximately 81% of the protons had energies between 7.8 and 8.8 MeV, $\sim$16% between 7.4 and 6.3 MeV, and $\sim$3% between 5.8 and 4.4 MeV. The spreads at all other energies were within the data point symbols.

B. Experimental Details for Double Heterojunction LEDs

Double heterojunction lot #4 LEDs were exposed to 9.5, 20, 63, 103, 200, and 500 MeV protons. For all energies all LEDs were exposed to the between 1.2 to 3×10^{12} p/cm^2. All beams were monitored for uniformity across the exposure area. This uniformity was within 10% for the 63, 103, and 200 MeV beams. The 9.5, 20 and 500 MeV fluence data was to be corrected for the nonuniformity.

Double heterojunction lot #3 LEDs were exposed to 9.5, 30, 63, 103, 225, and 500 MeV protons. For all energies all LEDs were exposed to the between 2 to 4×10^{11} p/cm^2. All beams were monitored for uniformity across the exposure area. This uniformity was within 10% for the all energies.

Using TRIM we estimate the spread in the proton energy due to shadowing from 1.3 mil gold bond wires, gold bonds, and the AlGaAs 40–80 μm N region epi-layer. For the 9.5 MeV proton beam, approximately 81% of the protons had energies between 8.3 and 8.9 MeV, $\sim$16% between 6.8 and 7.5 MeV, and $\sim$3% between 6.0 and 5.1 MeV. The spreads at all other energies are within the data point symbols.

IV. Output Power Dependence on Proton Fluence

As outlined earlier displacement damage effects that result in the creation of nonradiative recombination centers are the likely mechanism for output power degradation of LEDs. The result is a decrease in minority carrier lifetime. Direct measurement of the lifetime has been described in [22], [8].

In this study, we are not specifically interested in the absolute value of the damage factor, rather in its energy dependence. This can be determined by observing the relative change as a function of proton energy.

The measurement approach chosen for this study allowed for simple measurement of output power incident on a photodetector (see Section V). We employed a method described by Barnes *et al.* [1] to determine the damage factor from the output power measurements. In [1] the authors developed a series of relationships that relate changes in LED output power to fluence

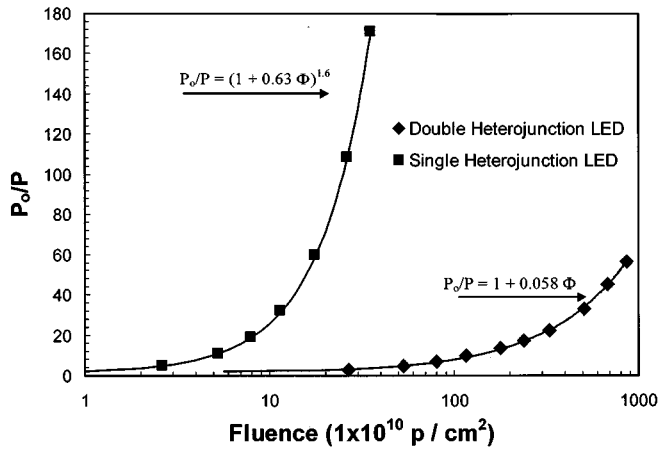

Fig. 6. Damage factors for single-heterojunction LEDs (solid squares) and double-heterojunction LEDs (solid diamonds), along with solid lines showing the best fits of the data to equation (1). Best fit relations for single-heterojunction devices are shown in the upper right of the plot, and for double-heterojunction devices at the lower left.

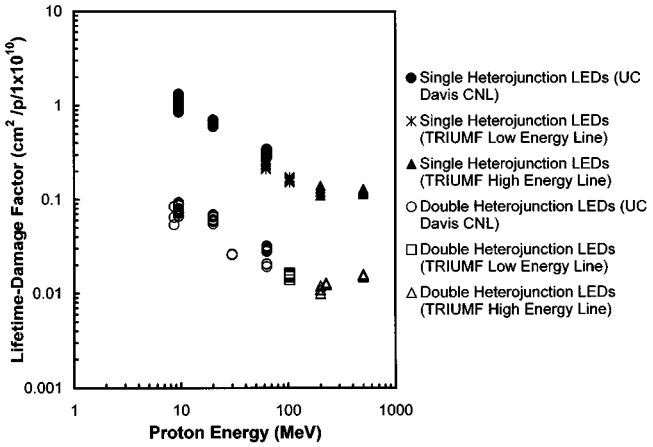

Fig. 7. Lifetime-damage-factor product values that give the best fit to equation (1) for single-heterojunction (upper curve) and double-heterojunction (lower curve) LEDs. Plotted values are for runs at all three beam lines and multiple lots irradiated to a variety of proton fluences.

(φ). These relationships depend on the initial lifetime (τ_o) and the damage factor (K). The general result of this work is given by:

$$\frac{P_0}{P} = (1 + \tau_0 K \varphi)^N \tag{1}$$

where P_o is the initial output power and P is the post-irradiation output power. In the current work, we fit this equation to experimental data using the lifetime-damage-factor product ($\tau_o K$) and N as fitting parameters.

As it turns out one can determine N if enough information is known about the LED and how it is used. The details of the parameters that determine N for a specific LED are given in [1]. We summarize them here; 1) N is defined by the distribution of the radiative recombination centers throughout the active region of the LED. A linear grading of recombination centers will give a different value for N than a uniform distribution of these centers. Protons create nonradiative centers, therefore the distribution of radiative centers is not effected by proton exposures. 2) N also depends on the current flow mechanisms that induce radiative recombination. An LEDs response to radiation will be different depending whether its the recombination current is dominated by diffusion current versus space-charge current. 3) Finally, the value of N depends on whether the device is used with a constant forward bias or a constant forward current. The important point to take away from this summary is that N does not depend on proton energy. So, determining N by any means will fix the value of N for all energies.

We chose to determine N experimentally, by estimating the value of $\tau_o K$ and N for each LED type using output power degradation data obtained on 21 LEDs of each type exposed at 20 MeV protons. These data were fit using equation 1 and the values for N were determined for all LEDs. Fig. 6 shows an example of this for each LED type. (The forward current was 4 mA, this prevented corruption of data due to injection current annealing.) The figure plots the output power ratio (P_o/P) as a function of fluence for the single heterojunction (squares) and double heterojunction LEDs (diamonds). The fluence is normalized to 1×10^{10} p/cm^2. The solid line associated with each data set is the best fit to the data. The equation of the best fit for each device type is given in the figure.

Using this type of analysis for the 21 LEDs of each type, we estimated the value for N. The value for the single heterojunction LEDs was found to be 1.63 with a standard deviation of 0.03. The value of N for the double heterojunction LEDs was 1.00 with a standard deviation of 0.04. The high degree of correlation arises from both the well behaved progression of damage with proton fluence and also with the tight grouping of the device-to-device variability in the sets of 21 samples used throughout the study. All devices behaved very similarly and no outliers were excluded from the analysis. These values for N will be used to fix the value of N in equation (1). Then the lifetime-damage-factor product $\tau_o K$ was determined at all test energies.

The data in Fig. 6 also demonstrate the relative sensitivity of each device type. These data show that the single heterojunction LEDs are much more sensitive than the double heterojunction devices. We also note that other studies [1], [7], [8], [17] have shown that amphoterically doped LEDs can be very sensitive to proton exposure on the same order as the single heterojunction LEDs used in our study. This places the sensitivity of the single heterojunction devices we examined among the least tolerant class of LED technologies used in commercially available optocouplers.

V. Output Power Dependence on Proton Energy

The determination of the dependence of power degradation on proton fluence makes it possible to investigate the dependence of the same quantity on proton energy. As mentioned previously—and as indicated by the excellent quality of the fits in Fig. 6—the value of N is independent of energy. This means that the energy dependence in equation (1) is contained in the lifetime-damage-factor product, $\tau_o K$. Fig. 7 shows the values of $\tau_o K$ giving the best fits to the data for single-heterojunction (upper curve, $N = 1.0$) and both lots of

the double-heterojunction devices (lower curve, $N = 1.63$) to equation (1). The plot contains several notable characteristics.

First, there is fairly good agreement in the data from different beam lines and different facilities. In particular, the data for 63 MeV protons from CNL and those for 62 MeV protons at TRIUMF overlap within experimental errors (although there seems to be a slight systematic bias toward greater damage [$\sim$30% on average] at the latter facility). Even more notable is the consistency over time of results from a given facility. The agreement of results for the two different lots (#3 and #4) of double-heterojunction devices, tested on different dates, indicates that if there are any systematic calibration errors, then they are at least self consistent. The overall consistency between various data sets suggests that systematic errors between facilities are unlikely to affect the qualitative or quantitative results of the current study.

Second, the fact that lots 3 and 4 yield similar values for $\tau_o K$, despite being irradiated to fluences different by factors of 6–7.5, suggests that, as expected, the damage factor-lifetime product is independent of fluence. Lastly, although the single-heterojunction devices sustain about an order of magnitude more damage than the double-heterojunction devices, the general shapes of the curves are quite similar. This similarity argues for a common damage mechanism at work for both sets of devices. This raises the question of whether damage in these devices can be described in terms of NIEL.

At the very least, different devices or technologies can be compared using a Figure of Merit approach like that outlined by Barnes *et al.* in reference [1], with the suggested Figure-Of-Merit (FOM) being

$$FOM = \frac{P_o}{JV\tau_o K} = \frac{\eta_p}{\tau_o K}, \tag{2}$$

where P_o is the initial power at current J and voltage V, and $\eta_p$is the device power efficiency. Using this FOM, the current data set makes clear that the single-heterojunction LEDs would need to be a factor of 10 more efficient than the double-heterojunction devices to compensate for their greater radiation-damage susceptibility.

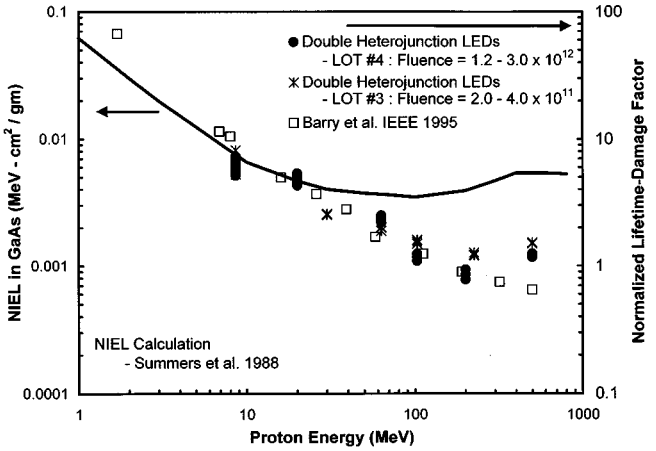

Fig. 8. Lifetime-damage-factor measurements for double-heterojunction devices (scaled to the right abscissa), normalized to agree with calculated NIEL values (solid line—scaled to the left abscissa) for 10 MeV protons. Data from the current study agree well with those from Barry *et al.*, except perhaps at the highest proton energies.

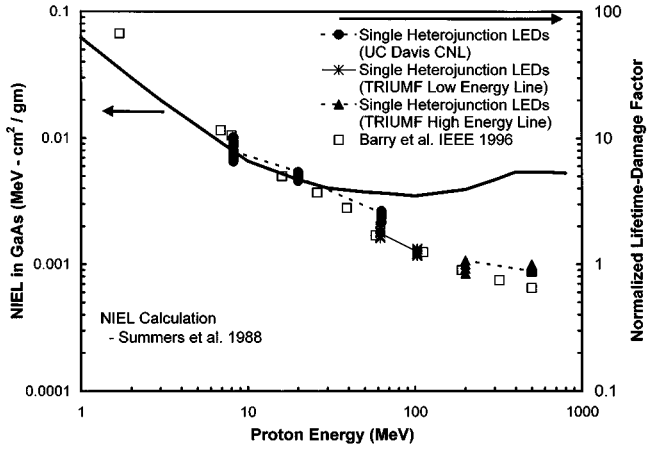

Fig. 9. Lifetime-damage-factor measurements for single-heterojunction devices (scaled to the right abscissa), normalized to agree with calculated NIEL values (solid line—scaled to the left abscissa) for 10 MeV protons. Data from the current study agree well with those from Barry *et al.*, except perhaps at the highest proton energies.

VI. Discussion

Figs. 8 and 9 compare $\tau_o K$ for single- and double-heterojunction LEDs, respectively, to NIEL as calculated by Summers *et al.* [12] (solid curve) and the results obtained by Barry *et al.* [8] (open squares in both plots). For these plots, the NIEL values are normalized to the values of $\tau_o K$ seen for the two device technologies at 10 MeV. It is clear that for both single- and double-heterojunction LEDs, the current data sets agree better with the experimental data from [8] than with the NIEL calculation [12]. (The significance of the slight upturn at high energy relative to the Barry data cannot be gauged at this time.)

The lack of consistency between calculated values of NIEL and the data presented here and in [8] argues against using the energy dependence of the NIEL to predict space-based performance of these LEDs from accelerator-based damage measurements at a single proton energy. Indeed, given the currently available experimental data, a conservative approach would be to measure damage at several energies and predict space-based performance by assuming the damage factor is piecewise continuous in proton energy. On the other hand, the similarity in the shapes of $\tau_o K$ vs. proton energy for both single- and double-heterojunction LEDs examined in the current work and for the data in [8] suggests that a "NIEL-like" approach may be possible using the proton-energy dependence observed in this experimental data.

Fig. 10 plots the various equivalent test fluence of 50 MeV or 200 MeV protons one would require to predict output power degradation due to damage from a combination of trapped and solar protons for a five year mission in a 600 km $\times$ 90 degree circular orbit. The equivalent fluence is given for NIEL and for the trend given by experimental data in Figs. 8 or 9. For lightly shielded applications, this figure shows a large difference in the estimated mission equivalent fluence depending on which energy dependence is assumed in the calculation. This discrepancy disappears for heavily shielded applications. This is because low energy protons are more easily stopped by shielding.

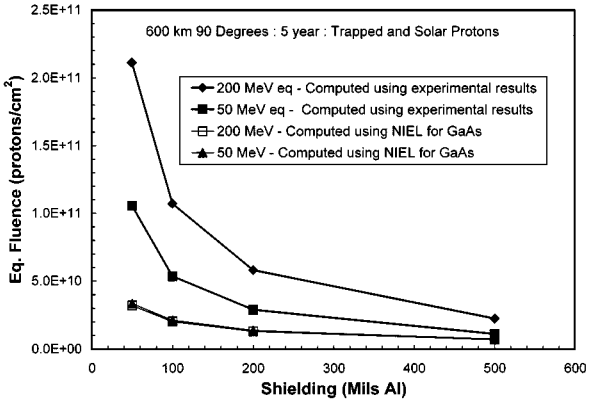

Fig. 10. On-orbit degradation for a mission (in this case 5 years, altitude 600 km, inclination 90°) can be predicted with a given fluence of protons, regardless of energy—provided displacement damage is proportional to NIEL. If damage follows experimental trends of Barry *et al.* proton beams of different energies require different equivalent proton fluences to inflict the same damage—especially for lightly shielded applications.

Based on the test data we present, if the normalization were made to damage from 200 MeV protons, then the NIEL correlation would lead to underestimation of the damage (or time to failure) by a factor of 7 for a device with 50 mils Al shielding. This magnitude of error could be disastrous. Normalization to test data at 50 MeV with the NIEL correlation shows a factor of 3 underestimation which is less dramatic, but significant nonetheless.

VII. Conclusions

Our study has undertaken a systematic examination and comparison of proton damage in two types of commercially available LEDs of different designs. Both are found in commercially available optocouplers favored by satellite designers, and both are based on GaAs material systems. Our results also presents a statistically significant comparison of single versus double heterojunction LEDs over the proton energy range from 9.5 to 500 MeV. Damage factors were carefully determined to assess their energy dependence versus that of the calculated NIEL for GaAs, and the results are similar in that the higher energy protons appear to be less damaging than expected. Though the trends with proton energy are similar, the relative tolerance is not so. The double heterojunction structure is significantly more tolerant to proton damage, while the single heterojunction device exhibits sensitivity similar to amphoterically doped LEDs which are noted for their problems in proton rich orbits.

With hardness assurance objectives in mind, we have critically examined the relative tolerance to displacement damage effects from proton bombardment and focused on the proton energy dependence of the degradation. Since such detailed investigations are usually out of scope for most flight projects, we compared our findings with typical hardness assurance approaches that sometimes rely on a single proton energy and correlation with the incident spectrum of proton energies using the energy dependence of the calculated nonionizing energy loss.

In part, our study was motivated by a review of the relevant literature, which we summarized here, for existing studies using the energy dependence of the calculated NIEL as a basis for correlating damage of various proton energies in GaAs based devices. We note a lack of consensus in the viability of the approach and cite several investigations that indicate that high energy protons, for which nuclear inelastic scattering is thought to be important, are not as damaging as lower energy protons for which the damage is dominated by Coulombic scattering.

Our study, spanning proton energies from 9.5 to 500 MeV, also indicates that higher energies are significantly less damaging than the NIEL correlation would suggest if the normalization were relative to low energy (e.g., 10 MeV protons). This discrepancy can lead to dramatically erroneous predictions if a single energy is used with the NIEL energy dependence to predict damage in a lightly shielded device. An indication of the severity of this effect was given in Fig. 10. Computing the single test energy equivalent fluence using NIEL would lead to underestimation of the damage by a factor of 3 to 7 for a device with 50 mils Al shielding depending on the proton energy selected for testing.

Out study was carried out on a specific set of LEDs (two types from a single source), we are cautious to generalize these results to other LEDs and other GaAs devices. However, we do note that our findings are consistent with other reported studies of GaAs based LEDs. With this in mind, we advise caution to anyone relying on the NIEL energy correlation and suggest the careful choice of test energy or preferably energies and as well as additional design margin to realistically bound the risk of on-orbit failures.

References

[1] C. E. Barnes and J. J. Wiczer, "Radiation effects in optoelectronic devices,", Sandia Rep. SAND84-0771, 1984.

[2] C. E. Barnes, "Radiation hardened optoelectronic components: Sources," in *Proc. SPIE*, vol. 616, 1986, pp. 248–252.

[3] B. H. Rose and C. E. Barnes, "Proton damage effects on light emitting diodes," *J. Appl. Phys.*, vol. 53, no. 3, pp. 1772–1780, March 1982.

[4] H. Lischka, H. Henschel, W. Lennartz, and H. U. Schmidt, "Radiation sensitivity of light emitting diodes, laser diodes and photodiodes," *IEEE Trans. Nucl. Sci.*, vol. 39, pp. 423–427, June 1992.

[5] B. G. Rax, C. I. Lee, A. H. Johnston, and C. E. Barnes, "Total dose and displacement damage in optocouplers," *IEEE Trans. Nucl. Sci.*, vol. 43, pp. 3167–3173, Dec. 1996.

[6] R. A. Reed, P. W. Marshall, A. H. Johnston, J. L. Barth, C. J. Marshall, K. A. LaBel, M. D'Ordine, H. S. Kim, and M. A. Carts, "Emerging optocoupler issues with energetic particle induced transients and permanent radiation degradation," *IEEE Trans. Nucl. Sci.*, vol. 45, pp. 2833–2841, Dec. 1998.

[7] A. H. Johnston, B. G. Rax, L. E. Selva, and C. E. Barnes, "Proton degradation of light-emitting diodes," *IEEE Trans. Nucl. Sci.*, vol. 46, pp. 1781–1789, Dec. 1999.

[8] A. L. Barry, A. J. Houdayer, P. F. Hinrichsen, W. G. Letourneau, and J. Vincent, "The energy dependence of lifetime damage constants in gaas leds for 1–500 mev protons," *IEEE Trans. Nucl. Sci.*, vol. 42, pp. 2104–2107, Dec. 1995.

[9] C. J. Dale, P. W. Marshall, E. A. Burke, G. P. Summers, and E. A. Wolicki, "High energy electron induced displacement damage in silicon," *IEEE Trans. Nucl. Sci.*, vol. 35, pp. 1208–1214, Dec. 1988.

[10] G. P. Summers, E. A. Burke, P. Shapiro, S. R. Messenger, and R. J. Walters, "Damage correlations in semiconductors exposed to gamma, electron and proton radiations," *IEEE Trans. Nucl. Sci.*, vol. 40, pp. 1372–1379, Dec. 1993.

[11] P. W. Marshall and C. J. Marshall, "Proton effect and test issues for satellite designers," *IEEE Nuclear and Space Radiation Effects Conf. Short Course*, p. I V-2-110, July 1999.

[12] E. A. Burke, C. J. Dale, A. B. Campbell, G. P. Summers, T. Palmer, and R. Zuleeg, "Energy dependence of proton-induced displacement damage in GaAs," *IEEE Tranc. Nucl. Sci.*, vol. 34, p. 1220, Dec. 1987.

[13] G. P. Summers, E. A. Burke, M. A. Xapsos, C. J. Dale, P. W. Marshall, and E. Petersen, "Displacement damage in GaAs structures," *IEEE Trans. Nucl. Sci.*, vol. 35, Dec. 1988.

[14] C. Carlone, M. Parenteau, A. Houdayer, P. Hinrichsen, and J. Vincent, "Photoluminescence study of gallium vacancy dfects in gallium arsenide irradiated by relativistic protons," *IEEE Trans. Nucl. Sci.*, vol. 44, p. 1856, Dec. 1997.

[15] T. F. Luera, J. G. Kelly, H. J. Stein, M. S. Lazo, C. E. Lee, and L. R. Dawson, "Neutron damage equivalence for silicon, silicon dioxide, and gallium arsenide," *IEEE Trans. Nucl. Sci.*, vol. 34, pp. 1557–1563, Dec. 1987.

[16] P. J. Griffin, J. G. Kelly, T. F. Luera, A. L. Barry, and M. S. Lazo, "Neutron damage equivalence in GaAs," *IEEE Trans. Nucl. Sci.*, vol. 38, pp. 1216–1224, Dec. 1991.

[17] S. C. Lee, Y. F. Zhao, R. D. Schrimpf, M. A. Neifeld, and K. F. Galloway, "Comparison of lifetime and threshold current damage factors for multi-quantum-well (MQW) GaAs/GaAlAs laser diodes irradiated at different proton energies," *IEEE Trans. Nucl. Sci.*, vol. 46, pp. 1797–1803, Dec. 1999.

[18] B. E. Anspaugh, "Proton and electron damage coefficients for GaAs/Ge solar cells," in *Proc. 22nd IEEE Photovoltaic Specialists Conf.*, 1992, pp. 1593–1598.

[19] M. Yamaguchi, C. Uemura, and A. Yamamoto, "Radiation damage in InP single crystals and solar cells," *J. Appl. Phys.*, vol. 55, pp. 1429–1436, 1984.

[20] R. J. Walters, M. A. Xapsos, G. P. Summers, and S. R. Messenger, "Analysis and modeling of the radiation response of space solar cells," in *1999 GOMAC Proc.*, Jan. 1999, pp. 434–437.

[21] J. F. Zeigler, J. P. Biersack, and U. Littmark, *The Stopping and Range of Ions in Solids*. New York: Pergamon, 1984.

[22] A. L. Barry, R. Maxseiner, R. Wojcik, M. A. Briere, and D. Braunig, "An improved displacement damage monitor," *IEEE Trans. Nucl. Sci.*, vol. 37, pp. 1726–1731, Dec. 1990.